Scientific Research Publishing

Journal of Transportation Technologies, 2023, 13, 689-707
https://www.scirp.org/journal/jtts
ISSN Online: 2160-0481
ISSN Print: 2160-0473

Comparison of Estimated Cycle Split Failures from High-Resolution Controller Event and Connected Vehicle Trajectory Data

Saumabha Gayen, Enrique D. Saldivar-Carranza, Darcy M. Bullock

Lyles School of Civil Engineering, Purdue University, West Lafayette, USA
Email: sgayen@purdue.edu, esaldiva@purdue.edu, darcy@purdue.edu

How to cite this paper: Gayen, S., Saldivar-Carranza, E.D. and Bullock, D.M. (2023) Comparison of Estimated Cycle Split Failures from High-Resolution Controller Event and Connected Vehicle Trajectory Data. *Journal of Transportation Technologies*, **13**, 689-707.
https://doi.org/10.4236/jtts.2023.134032

Received: August 24, 2023
Accepted: October 6, 2023
Published: October 9, 2023

Abstract

Current traffic signal split failure (SF) estimations derived from high-resolution controller event data rely on detector occupancy ratios and preset thresholds. The reliability of these techniques depends on the selected thresholds, detector lengths, and vehicle arrival patterns. Connected vehicle (CV) trajectory data can more definitively show when a vehicle split fails by evaluating the number of stops it experiences as it approaches an intersection, but it has limited market penetration. This paper compares cycle-by-cycle SF estimations from both high-resolution controller event data and CV trajectory data, and evaluates the effect of data aggregation on SF agreement between the two techniques. Results indicate that, in general, split failure events identified from CV data are likely to also be captured from high-resolution data, but split failure events identified from high-resolution data are less likely to be captured from CV data. This is due to the CV market penetration rate (MPR) of ~5% being too low to capture representative data for every controller cycle. However, data aggregation can increase the ratio in which CV data captures split failure events. For example, day-of-week data aggregation increased the percentage of split failures identified with high-resolution data that were also captured with CV data from 35% to 56%. It is recommended that aggregated CV data be used to estimate SF as it provides conservative and actionable results without the limitations of intersection and detector configuration. As the CV MPR increases, the accuracy of CV-based SF estimation will also improve.

Keywords

Split Failure, Connected Vehicle, Detector, Traffic Signal, Performance Measures, Trajectory Data

1. Introduction

The steady growth of vehicle miles travelled in the United States, from 2.62 trillion in 1999 to 3.15 trillion in 2022, has contributed to increased congestion in transportation systems [1]. A significant portion of these delays, between 5 to 10 percent, occur at traffic signals, which corresponds to nearly $23 billion in congestion costs when considering urban areas [2]. Thus, transportation agencies put great emphasis on traffic signal management, which is only possible with reliable performance measurements. Reliable and accurate signal performance measures allow agencies to identify intersections with congestion problems, analyze the cause of such problems, and develop location-specific solutions.

A popular traffic signal performance measure that provides insights on the level of congestion at a location of interest is split failure (SF) [3] [4]. A split failure event is when a traffic signal phase fails to serve its entire demand within one cycle, and the performance measure SF refers to the percentage of cycles in a time period which exhibit split failure. The SF value at a signal can be a useful metric to guide appropriate maintenance decisions [5] [6].

2. Literature Review

Previous research has focused on the development of traffic signal performance measures [4] [7] [8] [9] [10]. These performance measures allow practitioners to validate expected operations, assess demand, capacity, or progression, and quantify delay and travel time [4]. Signal performance measures are essential to transportation agencies for developing improvements [11].

Over the last decade, traffic signal performance has mainly been derived from controller-based automated traffic signal performance measures (ATSPMs). ATSPMs transform high-resolution controller event data into meaningful performance metrics that can readily be used by traffic engineers to prioritize maintenance and retiming activities, as well as conduct before-after studies. The Federal Highway Administration (FHWA) emphasized ATSPM implementation in round four of their Every Day Counts (EDC-4) initiative [12]. Additionally, FHWA released a cost-benefit evaluation, concluding that in most cases, the retiming savings are well worth the installation costs of ATSPM infrastructure [13]. High-resolution controller event data has not just been used to evaluate individual signals, but several studies have implemented this data with ATSPMs at the corridor and system level as well [14] [15] [16]. Widespread use of ATSPMs has led to commonly accepted performance measures such as arrival on green (AOG), green occupancy ratio (GOR), red occupancy ratio (ROR), and SF [4] [17].

Split failure events provide an indication that a traffic signal movement requires increased capacity either through signal retiming or capital investment. Freije *et al.* proposed a combination of phase termination cause and occupancy ratio thresholds during the green and red phases to determine when a split failure had likely occurred from high-resolution controller event data [18]. This method is used in the current study to predict when a split failure has occurred from controller event data. Li *et al.* expanded on this research by using the aforementioned split failure criteria and developing a scalable method to identify signal phases without sufficient green time [19]. A heuristic for reallocating split times using this approach was also developed shortly after [6].

Recently, connected vehicle (CV) trajectory data, which consists of frequent and accurate geospatial passenger vehicle information, has emerged as a viable alternative to generate traffic signal performance measures. Accordingly, there has been significant research on calculating signal performance measures and improving intersection efficiency using CV trajectory data [20] [21] [22] [23] [24]. A 2023 study has already used CV trajectory data to identify locations with signal retiming opportunity to reduce SF [5]. The current study employs a similar approach to predict when a split failure has occurred from CV trajectory data. Nevertheless, the major limiting factor of CV-based studies is the data set's low market penetration rate (MPR). Several studies that estimate CV MPR have been published over the last few years and have concluded that current MPR values are near 5% [25] [26] [27]. Regardless of this limitation, some studies have made signal operational decisions from aggregating CV-based data [28] [29].

3. Motivation and Objective

Estimating SF and other signal performance measures from high-resolution controller event data and CV trajectory data has been well-documented. Both data sources can provide useful performance measures given a sufficient time interval or sufficient CV trajectory sample size. However, controller-based SF estimation discrepancies resulting from different intersection and detector geometries have been discussed in previous research [7] [30]. Specifically, variation in detector length and vehicle arrival characteristics significantly impact the GOR and ROR used to identify phases with split failures.

In a recent study, Saldivar-Carranza *et al.* compared AOG estimations from high-resolution controller events (vehicle detection) and CV trajectories for 52 signalized intersections in Utah [31]. This study highlights the advantages of using CV data instead of ATSPMs to estimate AOG. It found that detector-based technique overestimated AOG by about 40% for periods with long queues or over-saturated conditions, suggesting that the CV-based technique is a better estimator under these conditions. However, no study was found to provide an in-depth comparison of SF estimations from controller- and CV-based techniques. Therefore, the current study compares SF estimations from both techniques, assesses the disagreement between the techniques, and identifies potential advantages of each data source.

The objective of this paper is to develop a methodology to compare split failures identified from high-resolution controller event data and CV trajectory data on a cycle-by-cycle basis. This will provide an idea on the degree of agreement between SF obtained from the two data sources and give agencies a preliminary indication of which source can provide more actionable results. Due to the relatively low MPR of CV data [27] and the intrinsic limitations of detector-derived estimations [30], there is some expected disagreement in identifying which cycles experience a split failure. It is expected that the number of split failures identified from CV data will be less than those identified from high-resolution data, as the latter virtually counts with 100% penetration and has more lenient criteria to estimate split failures. However, CV data is expected to provide more actionable results since it is based on the complete experience of traversing vehicles. This paper also explores two different methods of cycle aggregation and discusses the effect that they have on reducing split failure discrepancies.

4. Split Failure Identification by Data Source

A split failure at a signalized intersection occurs when a certain phase cannot serve its full demand within a cycle [12] [32]. Essentially, this happens when a vehicle must wait more than one full cycle length to cross the intersection.

Traditionally, split failure events have been associated with cycles. A cycle split fails when a vehicle reaches the stop bar detector during that cycle after having waited in the queue longer than the previous cycle length. However, split failure events can also be associated with individual vehicles. In this case, vehicles that have to stop during red at least twice before crossing the intersection are split failing vehicles. Therefore, a cycle can have more than one vehicle that experiences a split failure. In this paper, "split failure" will denote the occurrence of the event, whereas "SF" will refer to the performance measure given by the percentage of cycles that experience split failure.

Figure 1 shows a split failure at an intersection movement. The black vehicle indicated with the red arrow is stopped on red at 15:50:04 (**Figure 1(a)**), then attempts to cross during green, but has to stop on red for a second time at 15:51:17 (**Figure 1(b)**). Using the cycle definition, the cycle in which the vehicle reaches the stop bar detector split fails. Using the vehicle definition, this time interval has three vehicles that experience split failures, counting the black vehicle and the two white vehicles behind it. This section discusses how split failures are estimated from controller- and CV-based techniques.

(a)

(b)

Figure 1. Split failure occurrence at an intersection movement. (a) Stopped vehicle waiting for green time; (b) Stopped vehicle after green time.

4.1. High-Resolution Controller-Based SF Estimations

ATSPMs are derived from high-resolution signal controller data logs of time-stamped vehicle detector states (*i.e.*, on or off) and signal outputs (e.g., green, yellow, or red) for a given movement at an intersection. These data logs are then moved to servers for storage and software is then used to aggregate and analyze the data to produce usable metrics [12].

Using these logs, GOR and ROR during the first five seconds of red (ROR_5) can be calculated for each cycle at a signal movement by analyzing the amount of time that the detectors are occupied [18]. GOR calculation is shown in Equation (1), where O_g (s) is the sum of occupancy time during green for a cycle and T_g (s) is the green time for that cycle.

$$\text{GOR} = \frac{O_g}{T_g} \tag{1}$$

ROR_5 calculation is shown in Equation (2), where O_r (s) is the sum of occupancy time during the first five seconds of red.

$$\text{ROR}_5 = \frac{O_r}{5} \tag{2}$$

In this paper, a cycle split failure is identified from high-resolution controller event data when the green phase terminates by a max out or force-off, GOR is greater than or equal to 80%, and ROR_5 is greater than or equal to 80%. These criteria are commonly used in most event-based ATSPM systems [18].

Figure 2 shows a graphical representation of GOR and ROR_5 calculation. The detector state for a sample westbound-through (WBT) movement is shown in black and white, while the signal light phase is shown with green, yellow, and red. Two boxes are between the detector state and signal phase to show the percentage of time that the detector is occupied during green and the first five seconds of red. For this case, it is deemed that the cycle does not split fail as both GOR and ROR_5 are below 80%.

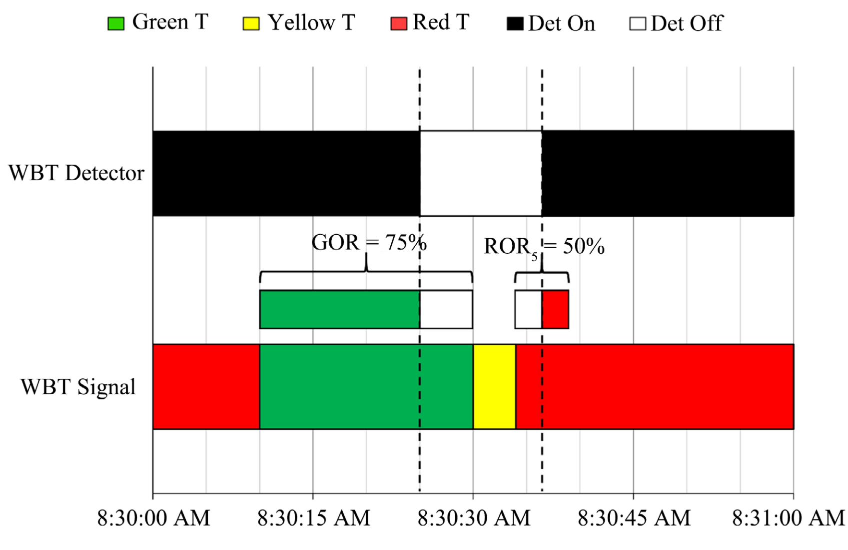

Figure 2. Graphical GOR and ROR_5 calculation from signal detector and phase [18].

4.2. CV Trajectory-Based SF Estimations

May 2023 Indiana CV trajectory data, with an estimated penetration rate near 5% [27], is used in this study. The data consists of individual passenger vehicle trajectory waypoints with a 3-s reporting interval and nominal 3-m spatial accuracy. Each waypoint has the following information: latitude, longitude, speed, heading, and an anonymous vehicle identifier.

From the CV data set, waypoints for each unique vehicle can be stitched to reconstruct its trajectory [3]. Waypoint headings near an intersection can then be used to identify the movement executed by each vehicle [33]. For each movement at a given intersection, a Purdue Probe Diagram (PPD) can be created, where each unique vehicle trajectory is plotted color-coded based on its number of stops on a time-space graph with the origin representing the far side of the intersection [3] [24].

Using a PPD, a split failure is visualized as a vehicle trajectory that stops at least twice [24]. **Figure 3** shows three examples of individual CV trajectories on a PPD. **Figure 3(a)** shows a vehicle that arrives on green and does not stop, **Figure 3(b)** shows a vehicle that stops once, and **Figure 3(c)** shows a vehicle that experiences a split failure as it stops twice. In this paper, a cycle is determined as split failing from CV data if there is at least one CV trajectory with two or more stops that reaches the upstream end of the stop bar detector within the cycle bounds [24].

5. Study Location

The signalized intersection used for this study is SR-32 and Union St (**Figure 4**) located in Westfield, IN, just north of Indianapolis. This signal is managed by the Indiana Department of Transportation (INDOT) and is a four-legged intersection with each approach having one through lane and one left-turn-only lane. The movement of interest is the WBT movement, for which there is a stop bar detector with a length of 51 feet. The time-of-day (TOD) period analyzed in this study is 8:00-9:00 AM for weekdays in May 2023.

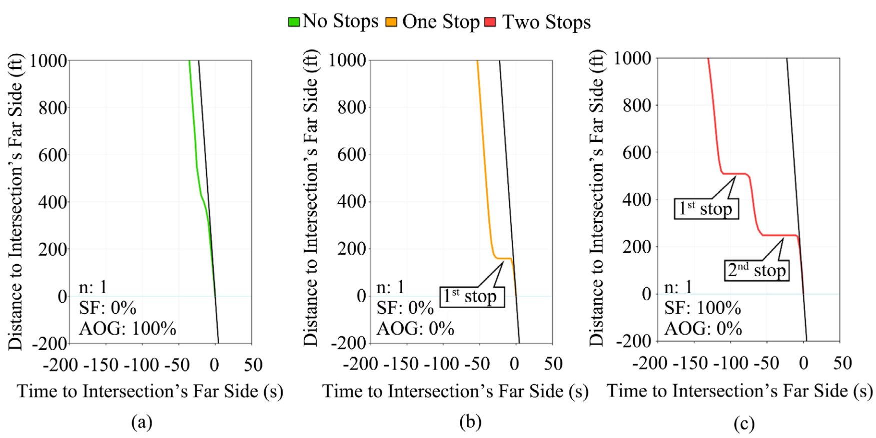

Figure 3. PPDs of vehicle trajectories with different number of stops. (a) No stops, AOG; (b) One stop; (c) Two stops, SF.

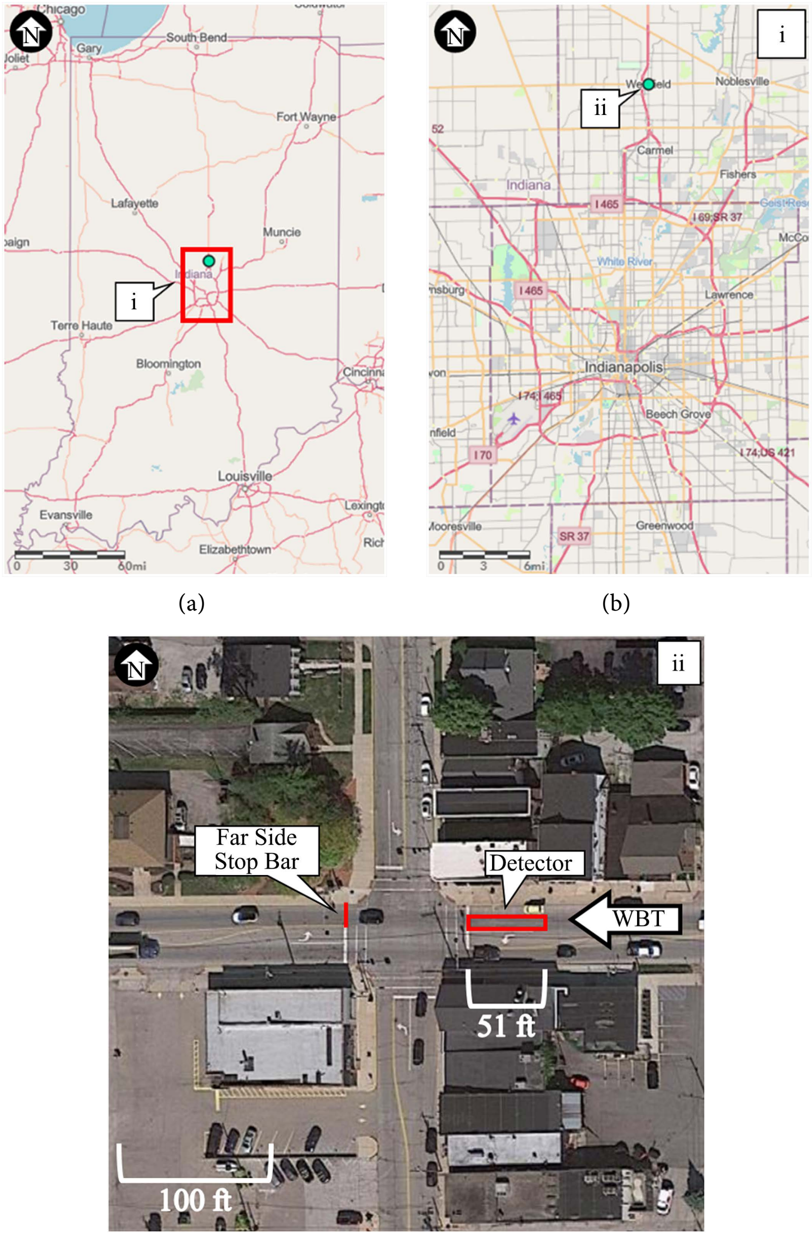

(a) (b)

(c)

Figure 4. Location and configuration of study intersection (map data: OpenStreetMap, Google). (a) Indiana; (b) Indianapolis; (c) SR-32 and Union St.

There are several reasons why SR-32 and Union St was chosen as the study location for the SF comparison. Most importantly, both high-resolution data and CV data were available for this intersection for the month of May 2023. Also, from previous analyses, it was determined that the WBT movement at this intersection experienced intermittent split failures and had a moderately high number of CV trajectories (with 720 unique samples). Finally, the selected WBT movement for this intersection has just one dedicated lane and associated detector, which simplifies the high-resolution SF analysis algorithm and its comparison with CV-based SF estimations.

6. Methodology

This section explains the methods used to compare SF estimations from high-resolution and CV data. CV data can provide the number of sampled vehicles that experience a split failure in a cycle. In contrast, high-resolution data can only offer a prediction of whether a cycle split fails based on the preset occupancy thresholds (Equation (1) and Equation (2)). Therefore, the comparison needs to evaluate the percentage of cycles that are estimated to split fail using both data sources.

6.1. High-Resolution and CV SF Estimation Agreement Categories

To assess the level of agreement between SF estimations at the evaluated movement, each signal cycle will be assigned to one of five categories depending on the high-resolution controller- and CV trajectory-based results. In the naming scheme for the categories, high-resolution has been abbreviated to "HR", and true and false are denoted with "T" and "F" after "HR" or "CV" to indicate whether a split failure has been estimated by that data source. The five categories are:

- High-resolution SF and CV SF (HRT-CVT): The cycle contains at least one CV trajectory and meets the split failure criteria for both techniques. This is an instance of agreement.
- High-resolution No SF and CV No SF (HRF-CVF): The cycle contains at least one CV trajectory and does not meet the split failure criteria for either technique. This is an instance of agreement.
- High-resolution SF and CV No SF (HRT-CVF): The cycle contains at least one CV trajectory and meets the split failure criteria for the high-resolution data but not for the CV data. This is an instance of disagreement.
- High-resolution No SF and CV SF (HRF-CVT): The cycle contains at least one CV trajectory and meets the split failure criteria for the CV data but not for the high-resolution data. This is an instance of agreement.
- No CV Trajectories (CVX): The cycle does not contain any CV trajectories. These cycles cannot be considered for comparison.

The first four categories can be tabulated on an agreement matrix to show the SF estimation relationship between the two data sources.

Figure 5 shows a comparison for seven cycles (c_1 through c_7) between 8:45-9:00 AM on Friday May 5th, 2023 for the WBT movement at SR-32 and Union St. Figure 5(a) depicts a TOD PPD with all observed CV trajectories for this time interval. Callout i points to a vertical gray line representing a cycle boundary (start of green). Callout ii points to a horizontal dashed black line representing the approximate distance where the stop bar detector begins. Each trajectory is assigned to the cycle in which it crosses this dashed line. Additionally, the signal phase state (*i.e.*, green, yellow, or red) is provided (callout iii). Figure 5(b) depicts a ROR_5 vs. GOR graph for the same seven cycles. All green phase terminations are caused by force-offs. It can be seen that split failure classifications are sensitive to small variations in the GOR threshold, as several cycles are clustered near the GOR = 80%, ROR_5 = 100% point.

Table 1 shows the corresponding agreement matrix for the cycles analyzed in Figure 5. Two of the seven cycles do not contain any CV trajectories (CVX), leaving five cycles that contain at least one trajectory. Out of these five cycles, three are categorized as HRT-CVT, one cycle is categorized as HRF-CVF, one cycle is categorized as HRT-CVF, and none of these cycles are categorized as HRF-CVT. High-resolution data gives four split failing cycles (80% SF), while CV data gives three (60% SF).

The HRT-CVF disagreement category is expected to occur frequently due to the low CV MPR. In the case that there is just one split failing vehicle in a cycle, it is likely that both GOR and ROR_5 will be high and the cycle will be indicated to split fail by high-resolution data. However, the probability that this vehicle is a CV and that its trajectory will be observed is simply the MPR of 5%. Accordingly, it is expected that SF estimated from high-resolution data (HRT) will be significantly greater than SF calculated from CV data (CVT).

The HRF-CVT disagreement is less common but can occur due to a few factors. One factor is that the detector occupancy thresholds used, in this case 80%

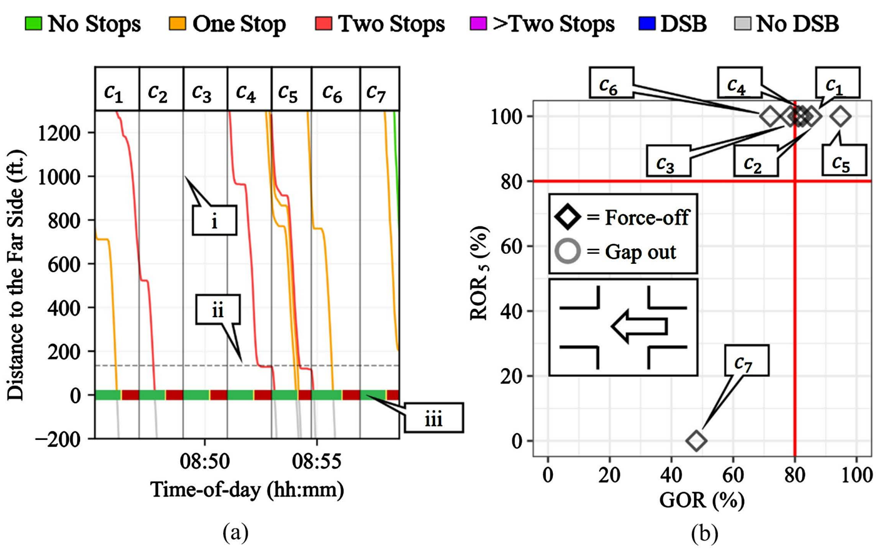

Figure 5. CV and high-resolution SF evaluation for 8:45-9:00 AM on Friday May 5th, 2023. (a) CV-based TOD PPD; (b) Controller-based ROR_5 vs. GOR.

Table 1. CV and high-resolution SF agreement matrix for all cycles in 8:45-9:00 AM on Friday May 5th, 2023.

	HRT	HRF	Total
CVT	3 (60%) c_2, c_4, c_5	0 (0%)	3 (60%)
CVF	1 (20%) c_1	1 (20%) c_6	2 (40%)
Total	4 (80%)	1 (20%)	5 (100%)

Note: 5 out of 7 cycles have at least 1 CV trajectory.

for both GOR and ROR_5, may be too high for the given intersection. For instance, the cycle could have operated just in over saturated conditions, such that there was just one split failing vehicle, which happened to be a CV, but either the GOR or ROR_5 values were just below the selected threshold. Another factor is inadequate detector length to account for unusual traffic scenarios, especially red light running. Red light running can decrease the ROR_5 value as there may be a gap in time until the first stopping vehicle behind red light running vehicles reaches the detector. For shorter detectors, this time gap will be greater, and the subsequent ROR_5 values will be lower.

6.2. Data Aggregation

Adequate sampling is required to correctly represent the real state of what is being measured. This concept is based on the Nyquist-Shannon sampling theorem [34], which states that a sufficient sampling rate to reconstruct a function is at least two times its highest frequency. Even though this theorem is not directly applicable to the estimation of traffic signal performance from CV data, the concept that additional samples can more accurately represent on-the-ground conditions still applies.

An approach likely to reduce discrepancies between SF estimations is to increase the representativeness of CV data by aggregating trajectories from different time periods. The effects that data aggregation has on SF results are evaluated by analyzing two different time periods: 8:00-9:00 AM for the four Fridays in May 2023, and 8:00-9:00 AM for May 1st through May 5th, 2023. The first period provides 29 cycles for four days, which is a total of 116 cycles that can be considered. These cycles are aggregated by day-of-week (DOW) to obtain 29 aggregated cycles for analysis, each containing information of the four corresponding cycles from each Friday. The second period provides the first 28 cycles for five days, which is a total of 140 cycles that can be considered. These cycles are longitudinally aggregated by TOD such that every four continuous cycles are grouped together. This method provides 35 aggregated cycles for analysis.

The SF criteria for the aggregated cycles are as follows:

- High-resolution data: If any of the four cycles in an aggregated cycle group are indicated to split fail, the aggregated cycle is also categorized as split failing.
- CV data: If any of the four cycles in an aggregated cycle group contains a trajectory that stops at least twice, the aggregated cycle is identified as split failing.

The two different aggregation methods, DOW and TOD, are used to consider both discontinuous and continuous time intervals. Both methods of aggregation in groups of four are done to see how either higher CV representativeness or larger time intervals impact the reliability of SF estimations.

7. Results

This section presents the resulting agreement matrices for both periods, the four

Fridays in May 2023 and May 1st through May 5th, 2023, for both individual cycles and aggregated cycles. Accompanying figures showing the aggregation by DOW and aggregation by TOD schemes are also included. For all four analysis scenarios, it is observed that SF estimations obtained from CV trajectory data are much lower than those obtained from high-resolution controller event data.

7.1. Four Fridays in May 2023

Individual Cycles

Figure 6 compares CV trajectories with detector occupancy ratios for seven cycles roughly in the 8:45-9:00 AM period for each Friday in May 2023. Figure 6(a) is a replica of Figure 5. For this time period, there is approximately one CV trajectory observed for each cycle. Table 2 shows the agreement matrix for the entire 8:00-9:00 AM period for the four Fridays without aggregation.

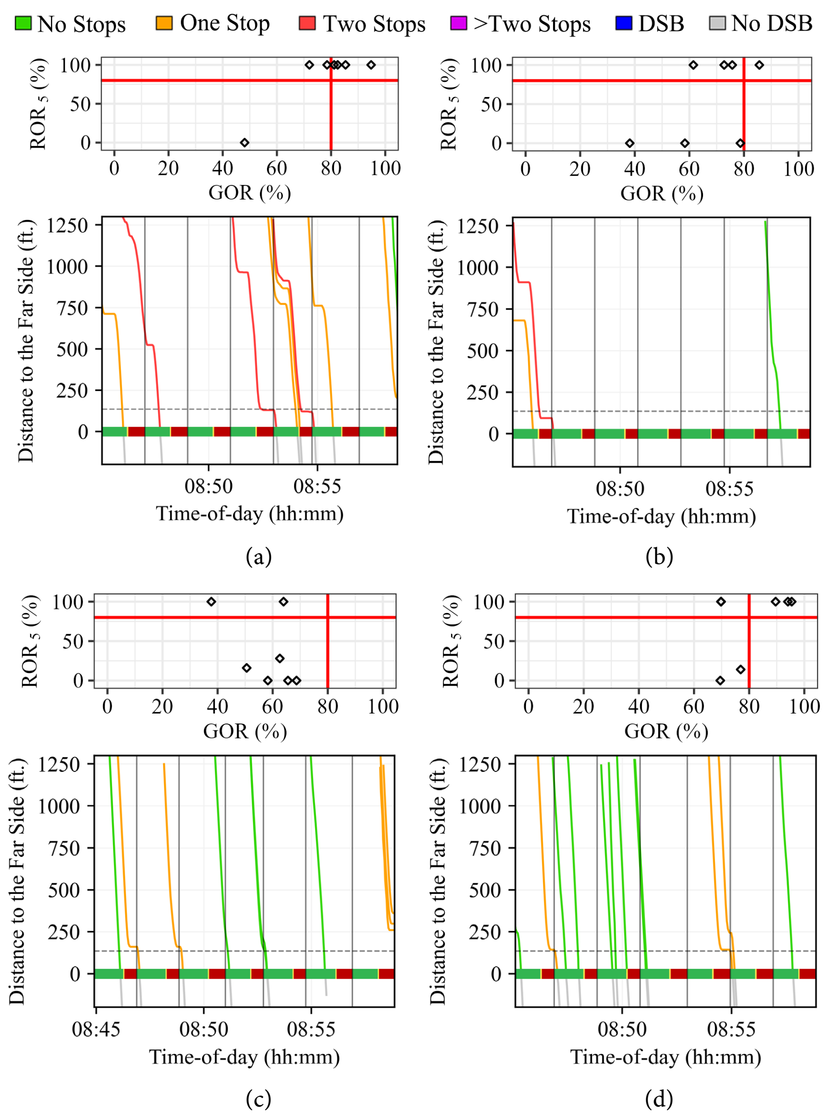

Figure 6. SF evaluations for all cycles in 8:45-9:00 AM for four Fridays in May 2023. (a) May 5th, 2023; (b) May 12th, 2023; (c) May 19th, 2023; (d) May 26th, 2023.

Table 2. CV and high-resolution SF agreement matrix for all cycles in 8:00-9:00 AM for four Fridays in May 2023.

	HRT	HRF	Total
CVT	13 (20.0%)	5 (7.7%)	18 (27.7%)
CVF	24 (36.9%)	23 (35.4%)	47 (72.3%)
Total	37 (56.9%)	28 (43.1%)	65 (100%)

Note: 65 out of 116 cycles have at least 1 CV trajectory.

Cycles Aggregated by Day-of-Week

Figure 7 shows all of the trajectories depicted in Figure 6 aggregated by DOW onto one PPD for the 8:45-9:00 AM period. Essentially, the first cycle in each subfigure in Figure 6 is combined as the first aggregate cycle (ac_1) in Figure 7, and the same is done for the other cycles. For this time period, five of the seven aggregated cycles are identified as high-resolution split failures, but only four of them contain a split failing CV trajectory. Table 3 shows the agreement matrix for the entire 8:00-9:00 AM period for the aggregated cycles of all four Fridays.

7.2. May 1st through May 5th, 2023

Individual Cycles

Table 4 shows the agreement matrix for the entire 8:00-9:00 AM period for May 1st through May 5th, 2023 without aggregation. The last cycle of each day is excluded for the eventual comparison with the aggregated cycles, which are groups of four cycles.

Cycles Aggregated by Time-of-Day

Figure 8 shows a PPD of all trajectories in the entire 8:00-9:00 AM period for Friday July 5th, with cycles aggregated by TOD, where each four adjacent cycles are grouped together. The aggregated cycle boundaries are shown by the solid black vertical lines, with the thin gray vertical lines representing each individual cycle boundary. For this day, all seven aggregated cycles are identified as high-resolution split failures, but only five of them contain a split failing CV trajectory. Table 5 shows the agreement matrix for the entire 8:00-9:00 AM period for all aggregated cycles in May 1st through May 5th.

8. Effect of Cycle Aggregation

Table 6 shows the effect of aggregation on the percentage of cycles in each category for both periods considered. The column headings are color-coded such that green indicates agreement and red indicates disagreement between SF estimations from both techniques. The second to last column is the percentage (P) of cycles that contain a split failing CV trajectory given that they are identified as split failing by high-resolution data (CVT|HRT). It is calculated as:

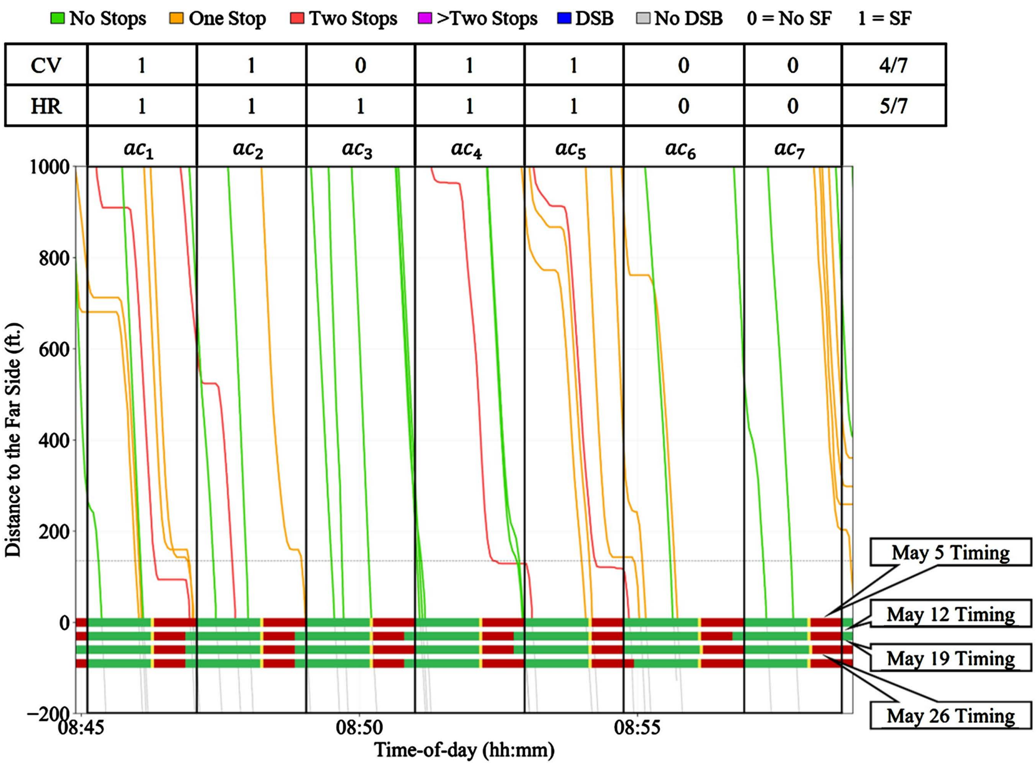

Figure 7. SF evaluation of cycles aggregated by DOW for 8:45-9:00 AM for four Fridays in May 2023.

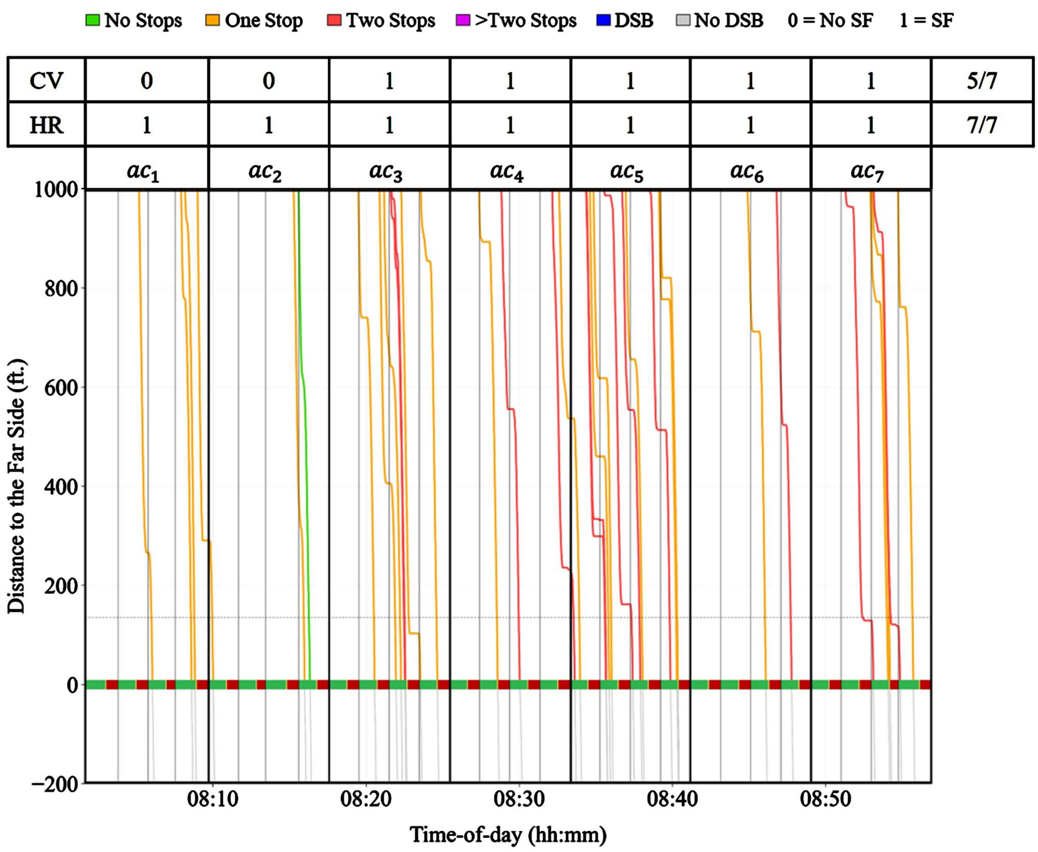

Figure 8. SF evaluation of cycles aggregated by TOD for 8:00-9:00 AM on Friday May 5th, 2023.

Table 3. CV and high-resolution SF agreement matrix for cycles aggregated by DOW in 8:00-9:00 AM for four Fridays in May 2023.

	HRT	HRF	Total
CVT	14 (48.3%)	1 (3.4%)	15 (51.7%)
CVF	11 (37.9%)	3 (10.3%)	14 (48.3%)
Total	25 (86.2%)	4 (13.8%)	29 (100%)

Note: 29 out of 29 aggregated cycles have at least 1 CV trajectory.

Table 4. CV and high-resolution SF agreement matrix for all cycles in 8:00-9:00 AM for May 1st through May 5th, 2023.

	HRT	HRF	Total
CVT	14 (14.0%)	1 (1.0%)	15 (15.0%)
CVF	41 (41.0%)	44 (44.0%)	85 (85.0%)
Total	55 (55.0%)	45 (45.0%)	100 (100%)

Note: 100 out of 140 cycles have at least 1 CV trajectory.

Table 5. CV and high-resolution SF agreement matrix for cycles aggregated by TOD in 8:00-9:00 AM for May 1st through May 5th, 2023.

	SF	No SF	Total
SF	11 (31.4%)	0 (0.0%)	11 (31.4%)
No SF	20 (57.1%)	4 (11.4%)	24 (68.6%)
Total	31 (88.6%)	4 (11.4%)	35 (100%)

Note: 35 out of 35 aggregated cycles have at least 1 CV trajectory.

Table 6. CV and high-resolution SF agreement by category.

Time Period	Cycle Analysis Approach	$P_{\text{HRT-CVT}}$	$P_{\text{HRF-CVF}}$	$P_{\text{HRT-CVF}}$	$P_{\text{HRF-CVT}}$	$P_{\text{CVT}\mid\text{HRT}}$	$P_{\text{HRT}\mid\text{CVT}}$
Four Fridays in May	Individual	20.0%	35.4%	36.9%	7.7%	35.1%	72.2%
	Aggregated by DOW	48.3%	10.3%	37.9%	3.5%	56.0%	93.3%
May 1st-5th	Individual	14.0%	44.0%	41.0%	1.0%	25.5%	93.3%
	Aggregated by TOD	31.4%	11.4%	57.0%	0.0%	35.5%	100%

$$P_{\text{CVT|HRT}} = \frac{P_{\text{HRT-CVT}}}{P_{\text{HRT-CVT}} + P_{\text{HRT-CVF}}} \tag{3}$$

The last column is the percentage of cycles that are identified as split failing by high-resolution data given that they contain a split failing CV trajectory (HRT|CVT). It is calculated as:

$$P_{\text{HRT|CVT}} = \frac{P_{\text{HRT-CVT}}}{P_{\text{HRT-CVT}} + P_{\text{HRF-CVT}}} \tag{4}$$

Low to moderate $P_{\text{CVT|HRT}}$ values confirm the expectation that the CV-based approach often misses split failures obtained from high-resolution data. This is primarily due to the low CV MPR and the corresponding low probability of sampling a split failing vehicle. However, the higher $P_{\text{HRT|CVT}}$ suggest that if a split failure is identified from CV data, it is likely to also be identified from high-resolution data, since a vehicle that stops at least twice before crossing will likely indicate congestion and produce high detector occupancy ratios. For the four Fridays in May, aggregation by DOW increases $P_{\text{CVT|HRT}}$ from 35.1% to 56.0% and $P_{\text{HRT|CVT}}$ from 72.2% to 93.3%. For May 1$^{\text{st}}$ through May 5$^{\text{th}}$, aggregation by TOD increases $P_{\text{CVT|HRT}}$ from 25.5% to 35.5% and $P_{\text{HRT|CVT}}$ from 93.3% to 100%. The observed increase in percentage of HRT-CVT cycles, $P_{\text{CVT|HRT}}$, and $P_{\text{HRT|CVT}}$, and the observed decrease in percentage of HRF-CVT cycles, are positive results of cycle aggregation.

The observed decrease in percentage of HRF-CVF cycles and the observed increase in percentage of HRT-CVF cycles are unexpected results. This is likely because of the high-resolution aggregation criteria that only one out of four cycles in a group must be identified to split fail in order for the aggregated cycle to be identified as split failing. This requirement was used to avoid increasing the instances of HRF-CVT disagreement, which would occur if more than one out of four cycles had to be identified to split fail. However, in using this requirement, the chance that an HRF cycle would be grouped into an aggregated cycle defined as HRT is much higher than the chance that a CVF cycle would be grouped into an aggregated cycle defined as CVT. This led to the decreased percentage of HRF-CVF cycles and increased percentage of HRT-CVF cycles.

The results displayed in **Table 6** offer an indication of SF estimation agreement category percentages between high-resolution and CV data for a single intersection movement. Future research is necessary to examine whether these percentages are similar over a diverse set of intersections with varying demand and congestion levels. Furthermore, the SF values obtained from both data sources can be assessed to see if there is significant correlation.

9. Conclusions

This study compared SF estimations from high-resolution controller event data and CV trajectory data at an intersection near Indianapolis, Indiana. Controller-based SF estimations rely on preset thresholds for detector occupancy ratios and have intrinsic limitations that depend on intersection and detector configuration. CV-based SF estimations instead use vehicle trajectories to count the exact number of times vehicles stop during their approach to an intersection.

Two time periods were analyzed from 8:00 to 9:00 AM in May 2023: the four Fridays in the month and the five-day span of May 1st through May 5th. For each period, the effect of cycle aggregation on SF agreement between the two methods was analyzed. The results of this analysis led to the following key findings:

- When a cycle split failure is identified from CV data, it is usually also detected with high-resolution data ($P_{\text{HRT|CVT}}$ greater than or equal to 72.2% for all four analysis scenarios).
- When a cycle split failure is identified from high-resolution data, it is not always detected with CV data ($P_{\text{CVT|HRT}}$ between 25.5% and 56.0% for all four analysis scenarios). This is a frequent discrepancy due to low CV MPR.
- CV data rarely indicates a cycle split failure when high-resolution data does not ($P_{\text{HRF-CVT}}$ less than 7.7% for all four analysis scenarios). Generally, this is due to GOR and ROR_5 thresholds not well-calibrated for variations in detector length.
- Data aggregation by cycle improves the agreement percentage of split failures identified with one technique given that the event is identified with the other technique ($P_{\text{CVT|HRT}}$ improved from 35.1% to 56.0% and $P_{\text{HRT|CVT}}$ improved from 72.2% to 93.3% with aggregation by DOW, and $P_{\text{CVT|HRT}}$ improved from 25.5% to 35.5% and $P_{\text{HRT|CVT}}$ improved from 93.3% to 100% with aggregation by TOD).

The CV-based method provides conservative estimations as it usually underestimates SF, but due to its direct use of vehicle trajectories, results are more likely to represent actual split failure events. From an agency standpoint, although the CV MPR is currently too low for cycle-by-cycle analysis, SF estimations derived from aggregated CV data can provide an important screening tool for identifying signals with congestion challenges. It is therefore recommended that aggregated CV data be used to estimate SF as it provides actionable results without the limitations of intersection and detector configuration. As the CV MPR continues to increase, the accuracy of CV-based cycle SF estimation will also increase.

Acknowledgements

CV trajectory data for May 2023 used in this study was provided by Wejo Data Services, Inc. High-resolution controller event data for May 2023 used in this study was provided by the Indiana Department of Transportation (INDOT). This work was supported in part by the Joint Transportation Research Program and Pooled Fund Study (TPF-5(377)) led by INDOT and supported by the state transportation agencies of California, Connecticut, Georgia, Minnesota, North Carolina, Ohio, Pennsylvania, Texas, Utah, Wisconsin, plus the City of College Station, Texas, and the FHWA Operations Technical Services Team. The contents of this paper reflect the views of the authors, who are responsible for the

facts and the accuracy of the data presented herein, and do not necessarily reflect the official views or policies of the sponsoring organizations. These contents do not constitute a standard, specification, or regulation.

Author Contributions

The authors confirm contribution to the paper as follows: study concept and design: S. Gayen, E. Saldivar-Carranza, D. Bullock; data collection: S. Gayen; algorithm development: S. Gayen, E. Saldivar-Carranza; analysis and interpretation of results: S. Gayen, E. Saldivar-Carranza, D. Bullock, draft manuscript preparation: S. Gayen, E. Saldivar-Carranza, D. Bullock. All authors reviewed the results and approved the final version of the manuscript.

Data Accessibility

The data that support the findings of this study are available from the corresponding author, Saumabha Gayen, upon reasonable request.

Conflicts of Interest

The authors declared no potential conflicts of interest with respect to the research, authorship, and/or publication of this article.

References

[1] FHWA: Federal Highway Administration (2023) Estimated Vehicle-Miles of Travel by Region, May 2023 (in Billions).

[2] ITE (Institute of Technical Education) and NOCoE (National Operations Center of Excellence) (2019) Traffic Signal Benchmarking and State of the Practice Report.

[3] Saldivar-Carranza, E.D., Li, H., Mathew, J.K., Desai, J., Platte, T., Gayen, S., Sturdevant, J., Taylor, M., Fisher, C. and Bullock, D.M. (2023) Next Generation Traffic Signal Performance Measures: Leveraging Connected Vehicle Data. Purdue University, West Lafayette. https://doi.org/10.5703/1288284317625

[4] Day, C., Bullock, D., Li, H., Remias, S., Hainen, A., Freije, R., Stevens, A., Sturdevant, J. and Brennan, T. (2014) Performance Measures for Traffic Signal Systems: An Outcome-Oriented Approach. Purdue University, West Lafayette. https://doi.org/10.5703/1288284315333

[5] Saldivar-Carranza, E.D., Li, H., Platte, T. and Bullock, D.M. (2023) Systemwide Identification of Signal Retiming Opportunities with Connected Vehicle Data to Reduce Split Failures. *Transportation Research Record*: *Journal of the Transportation Research Board*. https://doi.org/10.1177/03611981231168844

[6] Li, H., Richardson, L.M., Day, C.M., Howard, J. and Bullock, D.M. (2017) Scalable Dashboard for Identifying Split Failures and Heuristic for Reallocating Split Times. *Transportation Research Record*, **2620**, 83-95. https://doi.org/10.3141/2620-08

[7] Smaglik, E.J., Bullock, D.M., Gettman, D., Day, C.M. and Premachandra, H. (2011) Comparison of Alternative Real-Time Performance Measures for Measuring Signal Phase Utilization and Identifying Oversaturation. *Transportation Research Record*, **2259**, 123-131. https://doi.org/10.3141/2259-11

[8] Day, C.M., Li, H., Sturdevant, J.R. and Bullock, D.M. (2018) Data-Driven Ranking of Coordinated Traffic Signal Systems for Maintenance and Retiming. *Transporta-*

tion Research Record, **2672**, 167-178. https://doi.org/10.1177/0361198118794042

[9] Mahajan, D., Banerjee, T., Rangarajan, A., Agarwal, N., Dilmore, J., Posadas, E. and Ranka, S. (2019) Analyzing Traffic Signal Performance Measures to Automatically Classify Signalized Intersections. *VEHITS* 2019—*Proceedings of the* 5*th International Conference on Vehicle Technology and Intelligent Transport Systems*, Heraklion, 3-5 May 2019, 138-147. https://doi.org/10.5220/0007714700002179

[10] Dobrota, N., Stevanovic, A., Mitrovic, N., Alshayeb, S. and Zlatkovic, M. (2023) Development and Evaluation of Performance Measures for Capacity Utilization of Traffic Signals. *Transportation Research Record*, **2677**, 1337-1355. https://doi.org/10.1177/03611981221104460

[11] Day, C., Bullock, D., Li, H., Lavrenz, S., Smith, W.B. and Sturdevant, J. (2015) Integrating Traffic Signal Performance Measures into Agency Business Processes. Purdue University, West Lafayette. https://doi.org/10.5703/1288284316063

[12] FHWA: Federal Highway Administration (2020) Automated Traffic Signal Performance Measures.

[13] Day, C., O'Brien, P., Stevanovic, A., Hale, D. and Matout, N. (2020) A Methodology and Case Study Evaluating the Benefits and Costs of Implementing Automated Traffic Signal Performance. https://rosap.ntl.bts.gov/view/dot/54064

[14] Day, C.M. and Bullock, D.M. (2020) Optimization of Traffic Signal Offsets with High Resolution Event Data. *Journal of Transportation Engineering*, *Part A*: *Systems*, **146**. https://doi.org/10.1061/JTEPBS.0000309

[15] Day, C.M., Emtenan, T., Mahmud, S. and Knickerbocker, S. (2021) Data Driven Identification of Candidates for Operational Improvement Final Report. https://intrans.iastate.edu/app/uploads/2021/11/data_driven_ID_of_operational_improvement_candidates_w_cvr.pdf

[16] Guadamuz, R., Tang, H., Yu, Z., Guler, S.I. and Gayah, V.V. (2022) Green Time Usage Metrics on Signalized Intersections and Arterials Using High-Resolution Traffic Data. *International Journal of Transportation Science and Technology*, **11**, 509-521. https://doi.org/10.1016/j.ijtst.2021.06.006

[17] FHWA: Federal Highway Administration (2013) Measures of Effectiveness and Validation Guidance for Adaptive Signal Control Technologies.

[18] Freije, R.S., Hainen, A.M., Stevens, A.L., Li, H., Smith, W.B., Summers, H., Day, C.M., Sturdevant, J.R. and Bullock, D.M. (2014) Graphical Performance Measures for Practitioners to Triage Split Failure Trouble Calls. *Transportation Research Record*: *Journal of the Transportation Research Board*, **2439**, 27-40. https://doi.org/10.3141/2439-03

[19] Li, H., Day, C.M., Sturdevant, J.R. and Bullock, D.M. (2016) Scaling Detailed High-Resolution Data Split Performance Measures to Statewide System Level Management. https://doi.org/10.5703/1288284316048

[20] Ilgin Guler, S., Menendez, M. and Meier, L. (2014) Using Connected Vehicle Technology to Improve the Efficiency of Intersections. *Transportation Research Part C*: *Emerging Technologies*, **46**, 121-131. https://doi.org/10.1016/j.trc.2014.05.008

[21] Feng, Y., Head, K.L., Khoshmagham, S. and Zamanipour, M. (2015) A Real-Time Adaptive Signal Control in a Connected Vehicle Environment. *Transportation Research Part C*: *Emerging Technologies*, **55**, 460-473. https://doi.org/10.1016/j.trc.2015.01.007

[22] Wolf, J.C., Ma, J., Cisco, B., Neill, J., Moen, B. and Jarecki, C. (2019) Deriving Signal Performance Metrics from Large-Scale Connected Vehicle System Deployment. *Transportation Research Record*, **2673**, 36-46.

https://doi.org/10.1177/0361198119838520

[23] Khadka, S., Li, P.T. and Wang, Q. (2022) Developing Novel Performance Measures for Traffic Congestion Management and Operational Planning Based on Connected Vehicle Data. *Journal of Urban Planning and Development*, **148**. https://doi.org/10.1061/(ASCE)UP.1943-5444.0000835

[24] Saldivar-Carranza, E., Li, H., Mathew, J., Hunter, M., Sturdevant, J. and Bullock, D.M. (2021) Deriving Operational Traffic Signal Performance Measures from Vehicle Trajectory Data. *Transportation Research Record*, **2675**, 1250-1264. https://doi.org/10.1177/03611981211006725

[25] Wong, W., Shen, S., Zhao, Y. and Liu, H.X. (2019) On the Estimation of Connected Vehicle Penetration Rate Based on Single-Source Connected Vehicle Data. *Transportation Research Part B*: *Methodological*, **126**, 169-191. https://doi.org/10.1016/j.trb.2019.06.003

[26] Hunter, M., Mathew, J.K., Li, H. and Bullock, D.M. (2021) Estimation of Connected Vehicle Penetration on US Roads in Indiana, Ohio, and Pennsylvania. *Journal of Transportation Technologies*, **11**, 597-610. https://doi.org/10.4236/jtts.2021.114037

[27] Sakhare, R.S., Hunter, M., Mukai, J., Li, H. and Bullock, D.M. (2022) Truck and Passenger Car Connected Vehicle Penetration on Indiana Roadways. *Journal of Transportation Technologies*, **12**, 578-599. https://doi.org/10.4236/jtts.2022.124034

[28] Day, C.M. and Bullock, D.M. (2016) Detector-Free Signal Offset Optimization with Limited Connected Vehicle Market Penetration: Proof-of-Concept Study. *Transportation Research Record*, **2558**, 54-65. https://doi.org/10.3141/2558-06

[29] Osama, O.A., Bakhit, P.R. and Ishak, S. (2021) Analysis of Queue Estimation Process at Signalized Intersections under Low Connected Vehicle Penetration Rates. *Canadian Journal of Civil Engineering*, **48**, 1398-1408. https://doi.org/10.1139/cjce-2020-0366

[30] Emtenan, A.M.T. and Day, C.M. (2020) Impact of Detector Configuration on Performance Measurement and Signal Operations. *Transportation Research Record*, **2674**, 300-313. https://doi.org/10.1177/0361198120912244

[31] Saldivar-Carranza, E.D., Li, H., Gayen, S., Taylor, M., Sturdevant, J. and Bullock, D.M. (2023) Comparison of Arrivals on Green Estimations from Vehicle Detection and Connected Vehicle Data. *Transportation Research Record*: *Journal of the Transportation Research Board*. https://doi.org/10.1177/03611981231168116

[32] National Academies of Sciences, Engineering, and Medicine (2020) Performance-Based Management of Traffic Signals. Transportation Research Board, Washington DC.

[33] Saldivar-Carranza, E.D., Li, H. and Bullock, D.M. (2021) Identifying Vehicle Turning Movements at Intersections from Trajectory Data. 2021 *IEEE International Intelligent Transportation Systems Conference* (*ITSC*), Indianapolis, 19-22 September 2021, 4043-4050. https://doi.org/10.1109/ITSC48978.2021.9564781

[34] Shannon, C.E. (1949) Communication in the Presence of Noise. *Proceedings of the IRE*, **37**, 10-21. https://doi.org/10.1109/JRPROC.1949.232969